ISABE-2015-20048

AN INVERSE DESIGN METHOD FOR CASCADE BLADES UNDER VISCOUS FLOW CONDITIONS

Zhiheng Wang, ZhiYong Ren, Guang Xi
School of Energy and Power Engineering, Xi'an Jiaotong University,
Xi'an, 710049, P.R. China
xiguang@mail.xjtu.edu.cn

Abstract

Most of the existing inverse design methods cannot deal with viscous effects properly. To solve this problem, an aerodynamic inverse blade shape design method for viscous conditions is developed and incorporated with the flow analysis software Fluent to build an inverse design platform. In this design method, the pressure distribution of the blade surface is prescribed as the target. The blade wall moves with a virtual velocity distribution, which is derived from the difference between the target and current pressure distribution, until the shape corresponding to the prescribed pressure is achieved. The dynamic mesh model and User-Defined Function are used to control the blade grids' movements. With the inverse design platform, the analysis and redesign of a turbine stator cascade and compressor diffuser cascade are conducted. The inverse design results show that the target pressure distribution is well satisfied, so the effectiveness of the inverse platform is validated. The flow condition of the turbine cascade and the diffuser cascade are also improved through the redesign.

Nomenclature

Symbols

F: convective momentum flux
V: virtual velocity distribution
c: chord length
n: vector normal to the blade surface
p: pressure
r: residential
s: displacement
t: time
u, v: x,y component of V
δ: variable change
Δ: target variable minus present value

Subscripts

g: grid
v: viscous
s: smoothing

Superscripts

d: target
v: virtual
j: sequence number of the grids

Acronyms

CFD: Computational Fluid Dynamics
RANS: Reynolds Averaged Navier-Stokes
UDF: User-Defined Function

Introduction

In recent decades, the development of Computational Fluid Dynamics (CFD) methods provides a powerful tool to the analysis and design of turbomachinery, and many commercial CFD programs have matured and applied successfully into the industry. However, aerodynamic design methods using CFD schemes progress far behind analysis methods. Many designers still use the "cut and try" method, in which the performance of the geometry is evaluated and then modified according to the empirical rules or experience. This method is usually inefficient and time-consuming.

For the past few years, the superior aerodynamic performance of the Controlled Diffusion Airfoils (CDA) and the Prescribed Velocity Distribution Airfoils (PVD) arouse the interest in the inverse design method. In situations where the required performance (such as the blades pressure loading or the pressure distribution) is known, the aerodynamic inverse design method may

be the best method to get the target blade shape. The inverse design method starts from an initial shape, then computes the flow field to find the difference between the current and the target parameter to modify the blade shape, repeats the process above until the target is reached. Due to its clear physical significance, low computational cost and easy control of aerodynamic parameters, the inverse design method has attracted widespread attention and also got extensive applications in the blade shape design.

The inverse design methods have been under a continuous development. With the limitation of analysis tools, the early inverse design methods are implemented by analyzing potential function equations or stream function equations(Lighthill[1], Hawthorne et al.[2]). In the last few decades, as the CFD methods progresses quickly, several researchers try to combine the inverse method with the Euler (Demeulenaere[3] , Dang[4]) and Navier-Stokes (Malone et al.[5])solvers. The inverse methods evolve from the 2-D potential flow to the inviscid but rotational flow, then the viscous flow. This evolution process makes most of the inverse methods contain the traces of an inviscid flow implementation, such as the flow tangency condition required on the blade surface (Damle et al.[6]). De Vito et al. [7] combined an Euler solver for the inverse design and a Navier-Stokes solver for the flow analysis to accomplish the inverse design process. The existing inverse design methods mostly use the inviscid assumptions or account for viscosity effects in an approximate manner, which makes the viscosity effects under the real physical conditions cannot be taken into account properly. Hence, these methods cannot be applied to the viscous flow directly. Therefore, the development of an inverse design method which can consider the viscosity effects properly has an important significance.

Thompkins et al. [8] presented an inverse method which modifies the blade surface grids by a virtual velocity distribution derived from the momentum fluxes balance. It does not involve the flow tangency condition so that it is suitable for the viscous flow, but it solves the problem as a quasi-steady problem and does not account for the blade movement in the formulation, which will produce calculating errors. Daneshkhah et al. [9] used a time accurate solution of the Unsteady Reynolds Averaged Navier-Stokes(URANS) equations and modifying the control equations to account for the grids movement, so that the method is fully consistent with the viscous flow assumption. The method is also used in the redesign of a low speed turbine (Roidl et al. [10]) and compressor stages (Arbabi et al. [11]).

In this work, the aerodynamic inverse design of blade shape under real viscous conditions is studied and applied. The inverse design method developed by Daneshkhah et al. [9] is improved and implemented by coupling with the commercial CFD software Fluent to build an aerodynamic inverse blade shape design platform. In the design platform, User-Defined Function (UDF) is used to connect the inverse method with the Fluent flow solver. Then the platform is used to redesign two 2D cascades in viscous conditions: a turbine cascade and a diffuser cascade. The study demonstrated that the present inverse design platform is capable to handle viscous inverse design problems.

Blade shape modification algorithm

The key procedure of the inverse method is how to calculate the virtual velocity distribution to modify the blade shape, that is, the blade shape modification algorithm. In the current method, the moving-wall boundary condition is used to replace the fixed-wall boundary condition, and then the blade surface grids move to approximate the target shape. The movement is controlled by a virtual velocity distribution derived from the balance of the momentum flux between the current and the target pressure distributions on the wall. This method is independent of the flow tangency condition, and thus it can be applied to a viscous flow.

In the flow field analysis module, Reynolds Averaged Navier-Stokes (RANS) equations are used, and in the design module, URANS equations written in the Arbitrary Lagrangian-Eulerian (ALE) form are used. Accounting for the grids movement, the conservative form of the two-dimensional URANS equations is

written as[11]:

$$\frac{\partial U}{\partial t}+\frac{\partial(F-F_g-F_v)}{\partial x}+\frac{\partial(G-G_g-G_v)}{\partial y}=0 \quad (1)$$

where U is the vector of conservative flow variables, F-F_g and G-G_g are the convective flux vectors relative to the moving grid, and F_v and G_v are the viscous flux vectors.

The transient convective momentum flux F on the blade surface which moves with a virtual velocity distribution $V=(u^v,v^v)$ has the following form:

$$F=\begin{bmatrix}(\rho u^v v^v+p)n_x+(\rho u^v v^v)n_y\\(\rho u^v v^v)n_x+(\rho u^v v^v+p)n_y\end{bmatrix} \quad (2)$$

where $n=(n_x,n_y)$ is the vector normal to the blade surface, ρ is the density, p is the pressure. Once the blade shape reaches the target shape corresponding to the target pressure distributions, the virtual velocities should vanish and the target momentum flux F^d yields

$$F^d=\begin{bmatrix}(p^d n_x)\\(p^d n_y)\end{bmatrix} \quad (3)$$

By equating the transient and the target momentum fluxes, F and F^d, the virtual velocity components in the x and y directions can be calculated as following:

$$v^v=\pm\left(\frac{n_y^2}{n_x^2+n_y^2}\frac{\left|p^d-p\right|}{\rho}\right)^{\frac{1}{2}}$$

$$u^v=v^v\frac{n_x}{n_y} \quad (4)$$

A positive difference between the target and present pressures on the suction side induces a positive virtual velocity and vice versa on the pressure side. As can be seen from Equation (4), the virtual velocity V is normal to the blade surface. For convenience, the chordwise direction of the blade is taken as x direction, and the wall motion is taken only in y direction. In order to ensure the inverse problem stability, the virtual velocities should be under relaxed when computing the corresponding wall displacement. The relaxation factor ω is expressed as:

$$\omega=\lambda\cdot\sqrt{\left|\Delta p\right|/\rho} \quad (5)$$

where λ is a constant and it is set to be 0.0003 for the subsonic flow in this method.

The wall displacement δs should be proportional to the virtual velocity but in the opposite direction to drive the virtual velocity to 0. δs is expressed as:

$$\delta s=-\omega v^v\delta t \quad (6)$$

where δt is the user defined unsteady physical time step. The new blade geometry is then constructed by adding the wall displacements to the old blade geometry grids, see Fig. 1:

$$y_{new}=y_{old}+\delta s \quad (7)$$

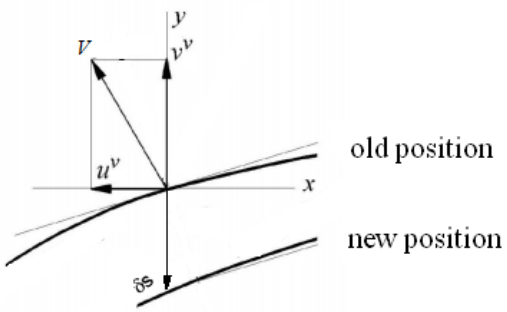

Fig. 1 Sketch of Grid Motion

In order to avoid the geometry oscillation, the resulting blade profile is smoothed by the following formulation:

$$y_{new}^j=y_{new}^j+\omega_s[\left|y_{new}^{j+1}-y_{new}^j\right|(y_{new}^{j+1}-y_{new}^j)+\left|y_{new}^{j-1}-y_{new}^j\right|(y_{new}^{j-1}-y_{new}^j)] \quad (8)$$

where ω_s is the smoothing coefficient and it is set to be 0.2 in the paper, j is the sequence number of the grids in blade surface.

Even though the smoothing is applied to the blade grids, it may still cause instability and divergence during iteration. As can be seen in the previous formula, the grid displacement is nearly proportional to the pressure difference, and the pressure difference may be very large near the leading edge and the trailing edge. Therefore, a further under relaxation is applied to the displacement here:

$$\delta y=\varepsilon^j\cdot(y_{new}^j-y_{old}^j) \quad (9)$$

where ε^j is the relaxation factor which is related to the position of the grid. ε^j can be expressed as:

$$\varepsilon^j=1-\left|\frac{2x^j}{c}-1\right| \quad (10)$$

where x^j is the x coordinate of the j^{th} grid point relative to the leading point, c is the chord length of the blade. δy is adopted as the actual grid

displacement to drive the grid point.

Although in Equation (2) the viscous flux terms were neglected, the wall is only driven by the balance of convective flux terms, the present inverse formulation works well for inviscid as well as viscous flows. It is believed that all the studied cases are correspond to high Reynolds number flows that the viscous fluxes are negligible compared with the convective fluxes [11].

Inverse design platform construction

In the inverse design platform, Fluent solver is used as the analysis module. By using the available commercial CFD software, the researchers needn't spend time on CFD analysis programming, and the computational accuracy and efficiency are ensured. In this design platform, the direct and inverse calculation are performed together, so that the flow field solution can be obtained directly when the inverse calculation converges without running the analyzing program again.

The blade shape modification algorithm is implemented into Fluent solver using a User-Defined Function (UDF). The inverse algorithm is written in C program files, and it works as the inverse design module. UDF and the dynamic mesh model are used to combine the blade shape modification algorithm with Fluent solver. The UDF program reads the flow field parameters from Fluent solver to calculate the grid displacement and returns the displacement to the dynamic mesh model. The dynamic mesh model drives the blade surface grid and the adjacent domain movement according to the command in UDF.

Inverse design process

The aerodynamic inverse design iterative process is conducted in three main steps, as shown in Fig. 2:

1) The initial blade shape is meshed and the flow field is analyzed in the steady CFD solver to get a converged solution as the initial input. The target pressure distribution is given under the same grid topology.

2) The inverse design module is conducted in the unsteady solver. At the beginning of each time step, the present grid points' positions and pressure distribution are read by UDF from the Fluent solver. The target pressure distribution is read from another file. The virtual velocities and grid displacements which drive the grid points to move are calculated according to the algorithm addressed above. Then the pressure residential on the blade surface grid is calculated as the convergence criterion (the L_2 norm of the grids' pressure difference between current and target pressure, see Equation (11)).

$$r = \sqrt{\sum (p^d - p)^2} \qquad (11)$$

When the residential change reaches a predetermined convergence level, the result is regarded to be converged and the present shape is regarded as the final result, or the calculation will go to the next step.

3) The UDF will return the grid displacements to the Fluent solver and dynamic mesh model is called to modify the control equation and to re-mesh the blade surface and adjacent grids. Then, the unsteady calculation is conducted automatically in Fluent solver until the convergence in current time step is reached. The solver goes to the next time step and repeats the previous procedures, until the pre-given convergence criterion is reached.

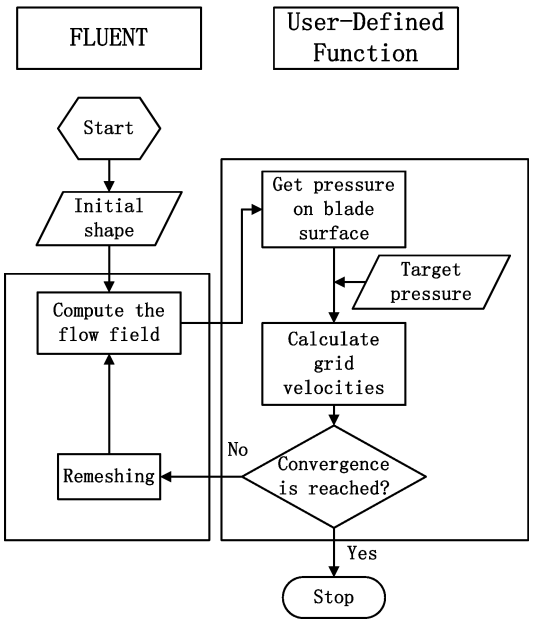

Fig. 2 Flow Chart of Inverse Design Method

Design variables

There are many groups of design variables can be used as the prescribed target variables in the inverse design method, such as the pressure distribution on pressure and suction sides, the pressure loading and thickness distribution, or the pressure distribution on suction side and thickness distribution. Because of the cases studied here are of a single blade row, it is easy for designers to impose a fixed inlet and outlet boundary conditions without expecting variations in the imposed values. Therefore, prescribing target pressure distribution on both pressure and suction sides is an easier approach. For those cases of multistage blade rows, due to the pressure on blade surface may vary, the prescribed pressure loading and thickness distribution may be a better choice.

In the choice of target pressure distribution, the virtual velocity is directly computed from the formula stated above and needs no transformation. However, because the blade thickness distribution is not prescribed, it may cause some structural problems. Therefore, some design constraints are necessary.

Inverse design constraints

For turbomachinery blade design, several geometric and non-geometric constraints have to be satisfied. Some of them are easily satisfied such as inlet Mach number, blade chord length. One of the main difficulties of inverse design procedure is to prescribe a reasonable target pressure distribution. An arbitrary choice of target pressure distribution may lead to a trailing edge crossover, an open blade shape, or any other unrealistic shape. In this method, the leading edge point and trailing edge point are fixed, and the grid point near them is linearly interpolated by the left and right grid points, while other grid points move as the modification computed by the inverse method above, as Fig.3 shows.

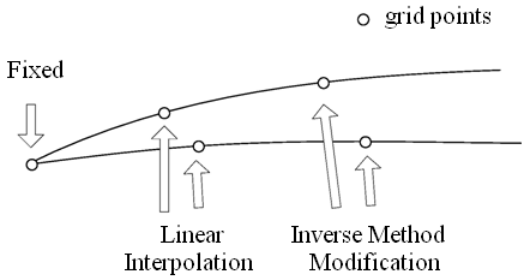

Fig. 3 Grid Points Movement Schematic

Inverse design implementation

The inverse design method is written in C program language according to Fluent defined macros, and then compiled and linked to the dynamic mesh model. The inverse method is attached to the domain where the grid modification is performed. The spring smoothing method of dynamic mesh model is adopted, in which the spring factor, boundary node relaxation, convergence tolerance are set to be 0.2, 0.2, 1×10^{-8} respectively. During the inverse design process, the dynamic mesh model and UDF are loaded automatically.

Validations of inverse design platform

Based on the established inverse design platform, the redesigns of a turbine stator cascade and a compressor diffuser cascade are conducted. The numerical simulation of the initial geometry is conducted first to get the initial flow field parameter. Then the blade surface pressure distribution is modified so as to be the target distribution. The goal is to optimize the aerodynamic performance of the two cases and to assess the usefulness and capability of the inverse design platform.

Inverse design of turbine cascade

The turbine cascade studied here is one blade passage of the stator cascades. The chord length and vane pitch of the cascade are 0.066m and 0.4m, respectively. The computational domain is extended in the upstream and downstream direction. A hybrid grid is adopted in the computational domain: a structured O-mesh is constructed around the blade to capture the flow in the boundary layer; the rest of the domain is filled with an unconstructed triangle mesh. The mesh near trailing

edge is shown in Fig. 4. The mesh consists of 33876 cells.

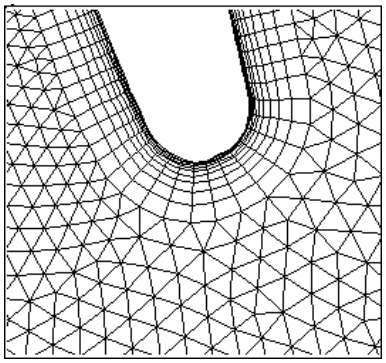

Fig. 4 Mesh near trailing edge

Then the CFD simulation of the cascade is conducted. The fluid is regarded as a perfect air and the Spalart-Allmaras turbulence model is adopted for the turbulence closure. The inlet total pressure and total temperature are respectively set to be 169600Pa and 293K. The inflow direction is axial. The outlet static pressure is 140000Pa; the blade surface is no-slip wall and the periodic boundary condition is set in two sides of the passage. The initial static pressure contour of the cascade is shown in Fig.5.

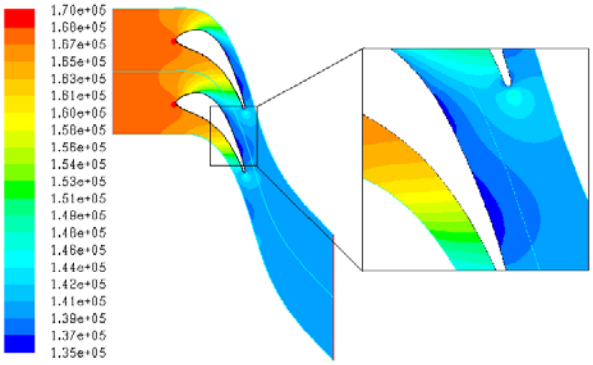

Fig. 5 Static Pressure Contour of Turbine Cascade

We can see from Fig.5 that there is a low pressure region in the middle chord length of the blade suction side, and occupies 2/3 of the suction surface. The pressure in that region fluctuates and it disturbs the flow in the passage. The low pressure region may cause adverse pressure gradient and induce the flow separation. Therefore, the target pressure distribution increases and smoothes the middle part of the suction side pressure distribution to improve the flow condition of the suction side.

The inverse design method was applied to the redesign of the turbine cascade. The unsteady time step is set to be 1×10^{-4}s at first, and generally increased in the iteration process, the final time step is 2.5×10^{-4}s. After 300 time steps, the residential reduces by nearly an order of magnitude and stop decreasing. The residential convergence curve is shown in Fig.6.

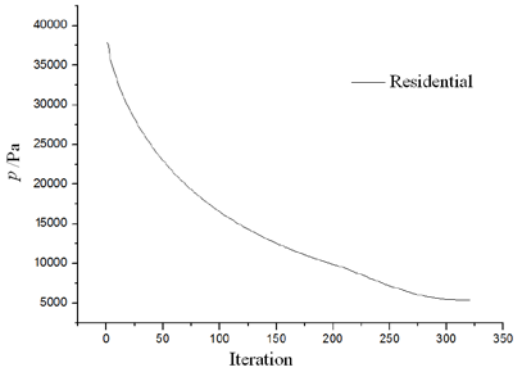

Fig. 6 Residential Convergence Curve

After the convergence, the computed shape and pressure distribution are obtained. The comparison of the computed, initial and target pressure distributions is shown in Fig.7, and Fig. 8 shows the computed resulting shape.

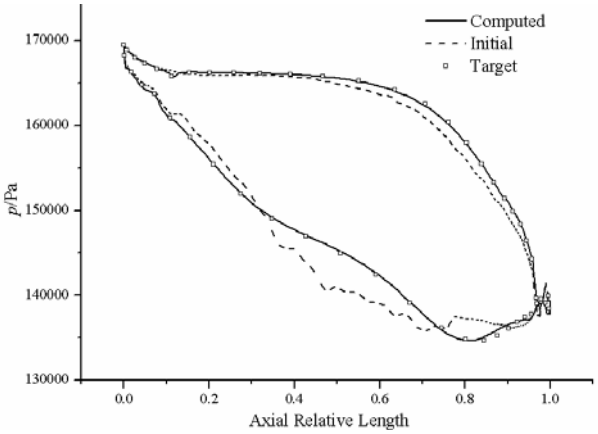

Fig. 7 Pressure Distribution Comparison of Turbine Cascade

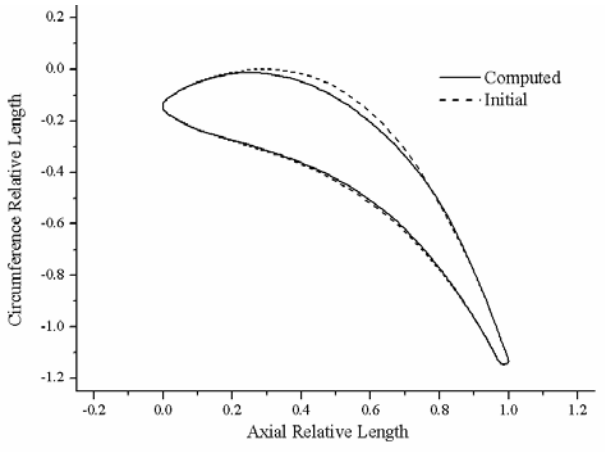

Fig. 8 Shape Comparison of Turbine Cascade

We can see that the target pressure distribution is well satisfied. Most of grids achieve the target pressure except for a very few points. The pressure in the suction side is smoothed. The blade shape of the middle suction side sinks thus decreases the flow turning angle of the suction surface, which contributes to the pressure rising. Fig.9 shows the comparison of static pressure contour between the initial and computed cascades. It can be seen that the low pressure region is reduced and the disturbance of the low pressure region to the passage flow is reduced. In general, the flow condition of the cascade is improved.

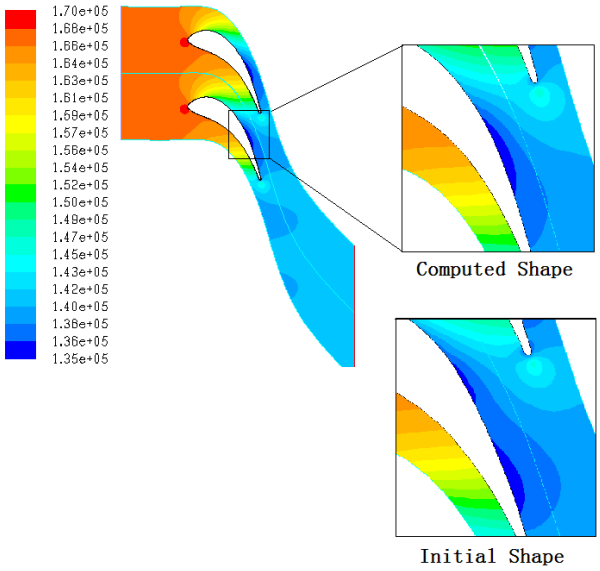

Fig. 9 Static Pressure Comparison of Turbine Cascade

The redesign of the turbine cascade validates the effectiveness and accuracy of the inverse design platform for the viscous case. After the redesign, the flow condition of the suction side is improved.

Inverse design of diffuser cascade

The second validation case is a vaned diffuser cascade of a high speed centrifugal compressor. The diffuser has an inlet radius of 87.475mm and an outlet radius of 147.3mm. The blade number is 22. As the previous case, a hybrid grid is applied. The mesh consists of 21020 cells.

Then the CFD simulation is conducted. The fluid material and the turbulence model remain the same. The inlet mass flow rate and total temperature are respectively set to be 5.4kg/s and 484.1K. The inflow direction is 24° deviation of the circumference direction, which is given by the CFD solution of the impeller outlet. The outlet static pressure is 484200Pa; the blade surface is no-slip wall and the rotational periodic boundary condition is set in two sides of the passage. The original static pressure contour of the cascade is shown in Fig.10.

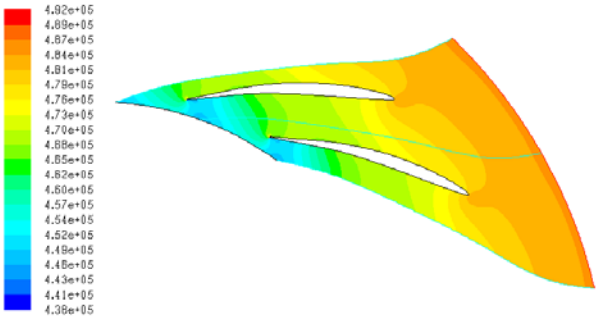

Fig. 10 Static Pressure Contour of Diffuser Cascade

As can be seen in Fig.10, the pressure of the concave side of the cascade inlet is very low, but the pressure of the convexity side is much higher. Furthermore, the pressure rise is mainly done in the fore part of the diffuser, but in the rear part of the passage, the pressure rise is little.

Therefore, the target pressure distribution increases the pressure of the concave side and decrease the convexity side to improve the flow condition of the diffuser inlet. According to the study of reference [12], the middle part of the pressure distribution is also modified.

The inverse design method was

applied to the redesign of the diffuser cascade. The unsteady time step is set to be 1×10^{-4}s firstly, and also gradually increased. The final time step is 3.5×10^{-4}s. After 600 time steps, the residential reduces by nearly an order of magnitude and the convergence is obtained. The residential convergence curve is shown in Fig.11.

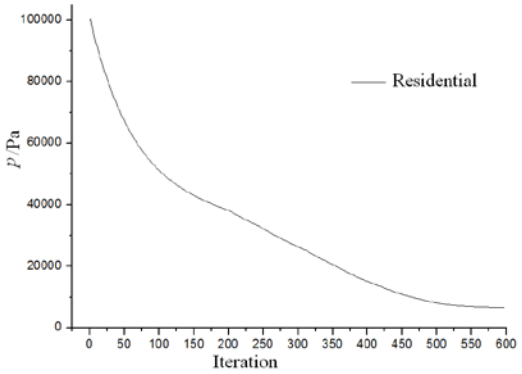

Fig. 11 Residential Convergence Curve

The comparison of the computed, initial and target pressure distributions is shown in Fig.12, and Fig. 13 shows the computed resulting shape. We can see that even though the target pressure distribution is quite different from the initial pressure, the target pressure distribution is quite well satisfied. The main blade loading position moves backward as prescribed. The computed shape in 10%-70% chord length of convexity side is sunken, which means the expansion ratio of the convexity side is increased, and that of the concave side is decreased. The maximum thickness of the cascade remains almost the same, which will not cause the strength problem.

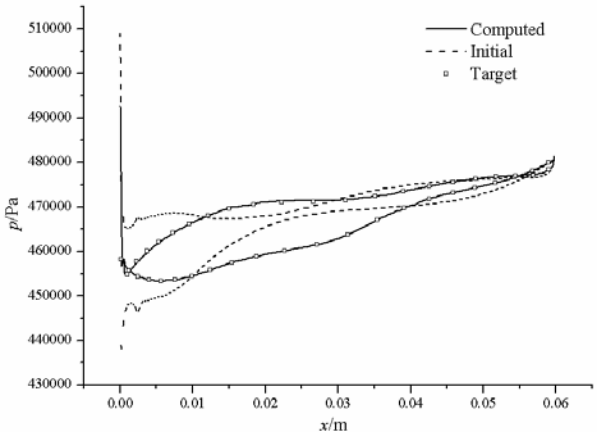

Fig. 12 Pressure Distribution Comparison of Diffuser Cascade

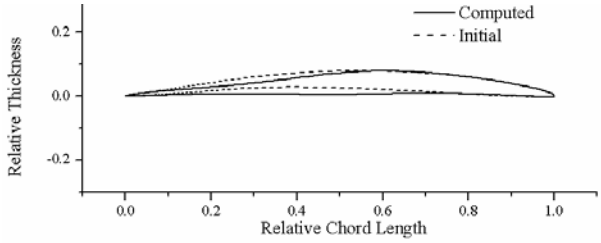

Fig. 13 Shape Comparison of Diffuser Cascade

Fig.14 shows the comparison of static pressure contour in the initial and computed cascades. It can be seen that the pressure difference of the two sides of the diffuser inlet is decreased. The pressure distribution near leading edge is more uniformed. The pressure rise is no longer concentrate on the inlet section, and it distributes more uniform along the flow path.

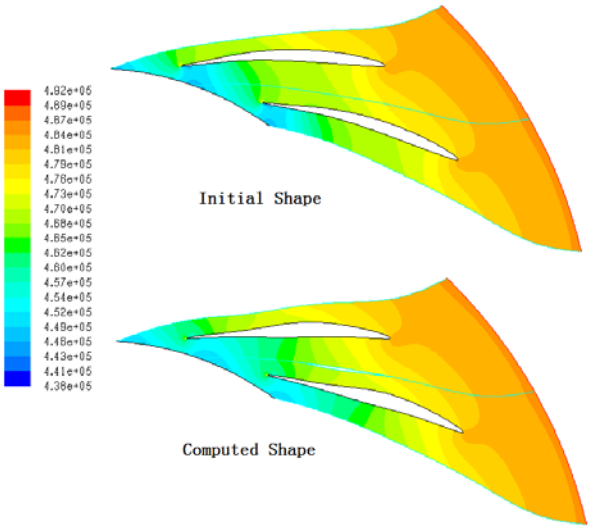

Fig. 14 Flow Field Comparison of Diffuser Cascade

In order to assess the aerodynamic performance of the diffusers before and after the inverse design, a quantitative comparison is carried out. The static pressure recovery coefficient C_{RC} and the total pressure loss coefficient C_{LC} are used as the comparison criterion. The expressions of C_{RC} and C_{LC} are as following:

$$C_{RC}=\frac{p_4-p_3}{p_{t3}-p_3} \tag{1}$$

$$C_{LC}=\frac{p_{t3}-p_{t4}}{p_{t3}-p_3} \tag{2}$$

where p_4 and p_3 are the static pressure of the outlet and inlet, and p_{t4} and p_{t3} are the total pressure of the outlet

and inlet. The comparison of the initial and designed cascades is listed in Tab. 1:

Tab. 1 Comparison of Initial and Designed Diffuser Cascades

	C_{RC}	C_{LC}
Initial	0.72077	0.036587
Designed	0.72557	0.034614
Change Rate/%	0.666	-5.393

As can be seen in Tab. 1, the static pressure recovery coefficient of the designed cascade is increased by 0.666%, and the total pressure loss coefficient decreases by 5.393%. Namely, the aerodynamic performance of the designed cascade is improved.

The redesign of the diffuser cascade validates the effectiveness of the inverse design platform for the viscous case again and improves the flow condition of the diffuser.

Conclusions

In this paper an aerodynamic inverse blade shape design method for viscous conditions is implemented into the commercial CFD software Fluent with the User-Defined Function to build an inverse design platform. In the current method, the moving-wall boundary condition is used to replace the fixed-wall boundary condition, and the movement is controlled by a virtual velocity distribution derived from the momentum flux balance between the current and the target pressure distributions on the wall. This method is independent of the flow tangency condition, and thus it can be applied to viscous flow.

Based on the established inverse design platform, the analysis and designs of a turbine stator cascade and a compressor diffuser cascade are conducted. For both cases, the computed blade surface pressure distributions are consistent with the target fairly well. The results validate the accuracy and usefulness of the platform and it can be used to optimize the aerodynamic performances of the cascades.

Acknowledgments

This work is financially supported by the National Nature Science Foundation of China under grant No. 51236006 and Xi'an Jiaotong University Scientific Research Support Program for New Staff under grant No. XJTU-HRT-002.

References

1 **Lighthill M**. A new method of two-dimensional aerodynamics design. Aeronautical Research Council: R&M2112, 1945.

2 **Hawthorne W**, **Wang C**, **Tan C**, et al. Theory of blade design for large deflections: part I—two-dimensional cascade.ASME Journal of Engineering for Gas Turbines and Power, 1984, 106(2): 346-353.

3 **Demeulenaere A**, **Van den Braembussche R**. Three-dimensional inverse method for turbomachinery blading design. ASME Journal of Turbomachinery, 1998, 120(2): 247-255.

4 **Dang T**, **Isgro V**. Euler-based inverse method for turbomachine blades part 1: two-dimensional cascades. AIAA Journal, 1995, 33(12): 2309-2315.

5 **Malone J**, **Narramore J**, **Sankar LN**. Airfoil design method using the navier-stokes equations. AIAA Journal of Aircraft, 1991, 28(3): 216-224.

6 **Damle S**, **Dang T**, **Stringham J**, et al. Practical use of three-dimensional inverse method for compressor blade design. ASME Journal of Turbomachinery, 1999, 121(2): 321-325.

7 **de Vito L**, **den Braembussche R**, **Deconinck M**. A novel two-dimensional viscous inverse design method for turbomachinery blading. ASME Journal of Turbomachinery,2003, 125(2): 310-316.

8 **Thompkins W**, **Tong S**. Inverse or design calculations for nonpotential flow in turbomachinery blade passages.ASME Journal for Engineering for Power, 1982, 104(2): 281-285.

9 **Daneshkhah K**, **Ghaly W**. An inverse blade design method for subsonic and transonic viscous flow in compressors and turbines.

Inverse Problems in Science and Engineering, 2006, 14(3): 211-231.

10 **Roidl B**, **Ghaly W**. Redesign of a low speed turbine stage using a new viscous inverse design method. ASME Journal of Turbomachinery, 2011, 133(1): 011009-011009-9.

11 **Arbabi A**, **Ghaly W**. Inverse design of turbine and compressor stages using a commercial cfd program. In: Proceedings of ASME Turbo Expo 2013. ASME Paper GT2013-96017, 2013. San Antonio:ASME, 2013.

12 **Zhang CL**, **Deng QH**, **Feng ZP**. Aerodynamic optimization design of vaned diffuser for centrifugal compressor under stage environment. Journal of Xi'an Jiaotong University, 2009, 43(11): 32-36. (In Chinese)